

# Effect of incorporating bioactive glass filler in resin infiltrant on the microhardness of demineralized enamel

Hila Hajizadeh<sup>1</sup>, Hossein Bagheri<sup>2</sup>, Aboubakr Azizzadeh<sup>3</sup>, Maryam Valizadeh<sup>4</sup>, Kimia Jafarpour<sup>3\*</sup>

## Abstract

**Objective:** This study aimed to evaluate the effect of incorporating different concentrations of 45S5 bioactive glass (BAG) as a filler into a resin infiltrant on the microhardness of demineralized enamel.

**Methods:** Forty bovine enamel samples were subjected to a pH-cycling protocol to induce artificial caries lesions. The teeth were randomly assigned to four groups (n = 10), based on the remineralizing treatment applied: G1: the commercial ICON® resin infiltrant (control); G2 and G3: experimental resin infiltrants containing 5 wt% (G2) and 2 wt% (G3) 45S5 bioactive glass; and G4: a filler-free resin infiltrant. Vickers microhardness was measured at depths of 50, 100, and 150 µm. The data were analyzed using two-way ANOVA ( $\alpha=0.05$ ).

**Results:** Both the type of resin infiltrant and lesion depth significantly influenced enamel microhardness ( $P<0.001$ ). ICON® consistently demonstrated the highest microhardness, significantly outperforming the other groups at all evaluated depths ( $P < 0.05$ ). Microhardness increased with depth in all groups, with significant differences observed between 50, 100, and 150 µm depths ( $P < 0.05$ ). Incorporation of Bioglass® 45S5 into the resin infiltrant was effective in enhancing microhardness, as compared to unfilled resin. The 5% concentration of Bioglass® 45S5 also caused a significant rise in microhardness compared to the 2 wt% at 50 µm depth ( $P<0.05$ ).

**Conclusions:** The commercial resin infiltrant (ICON®) consistently achieved the highest microhardness at all depths. The incorporation of Bioglass® 45S5 enhanced microhardness, with the 5 wt% group (G2) exhibiting superior performance compared with the 2 wt% group (G3) and the filler-free control (G4).

**Keywords:** Bioactive glass 45S5, Dental caries, Dental enamel, Dental resins, Hardness tests, Tooth remineralization

## Introduction

In the oral cavity, mineral dissolution and reformation of teeth occur continuously, maintaining a dynamic balance between demineralization and remineralization (1). When the pH in the oral environment falls, the saliva becomes undersaturated with respect to enamel minerals, leading to the dissolution of calcium and phosphate ions from hydroxyapatite crystals (2). Conversely, under neutral or higher pH conditions, the saliva becomes supersaturated, allowing these ions to

diffuse into the enamel and promote remineralization (2).

Prolonged exposure to acidic conditions can disrupt the natural balance of mineral exchange in enamel, leading to progressive mineral loss and the development of areas susceptible to further structural breakdown (3). These areas often appear as chalky, opaque regions, commonly referred to as early enamel caries or white spot lesions (WSLs). WSLs differ from sound enamel by their increased porosity and reduced mineral content (4). They are frequently observed in the gingival region of maxillary anterior teeth, particularly on maxillary canines and lateral incisors, and are often associated with inadequate plaque control (5).

Resin infiltration is a minimally invasive dental treatment that employs a low-viscosity, light-curing resin to penetrate the microporosities of demineralized enamel through capillary action (6). Early, non-cavitated enamel lesions with an intact surface layer are considered the primary candidates for resin infiltration (7). These lesions develop when mineral loss occurs beneath a

<sup>1</sup> Department of Restorative and Cosmetic Dentistry, School of Dentistry, Mashhad University of Medical Sciences, Mashhad, Iran.

<sup>2</sup> Dental Materials Research Center, Mashhad University of Medical Sciences, Mashhad, Iran.

<sup>3</sup> Student Research Committee, Mashhad University of Medical Sciences, Mashhad, Iran.

<sup>4</sup> Dental Research Center Mashhad University of Medical Sciences, Mashhad, Iran.

\*Corresponding Author: Kimia Jafarpour  
Email: [jafarpourkimia@gmail.com](mailto:jafarpourkimia@gmail.com)

Accepted: 10 October 2025. Submitted: 29 November 2025.



relatively intact surface layer, resulting in a porous subsurface zone (8, 9). By occluding subsurface pores and blocking acid diffusion pathways, resin infiltration arrests lesion progression and improves the optical properties of the affected enamel (6). This technique is particularly indicated when conventional remineralization therapies are insufficient due to limited ion diffusion into deeper lesion areas (10, 11). In such cases, resin infiltration provides dual benefits: arresting lesion progression and improving aesthetics by masking enamel opacity (9, 12).

Although conventional resin infiltrants are clinically effective, they present several limitations, including incomplete recovery of enamel microhardness, particularly in deeper lesion zones, limited subsurface penetration, and lack of intrinsic bioactivity (13-16). To overcome the intrinsic lack of bioactivity in conventional infiltrants, the incorporation of bioactive fillers such as 45S5 bioactive glass (BAG) has been proposed. BAG releases calcium, phosphate, and silica ions, promoting hydroxyapatite formation and enhancing mechanical reinforcement (17-19). Studies on BAG-modified infiltrants have reported improved microhardness, reduced water sorption, and enhanced mechanical stability (16, 20, 21).

However, most previous studies have focused on surface effects of BAG-modified infiltrants, and the influence of BAG concentration on subsurface microhardness at different lesion depths remains poorly understood. Therefore, this study aimed to evaluate the effect of incorporating different concentrations of 45S5 bioactive glass as a filler into resin infiltrant on the microhardness of demineralized enamel.

## Materials and methods

### *Ethics consideration*

This study was approved by the ethics committee of Mashhad University of Medical Sciences, Mashhad, Iran (IR.MUMS.DENTISTRY.REC.1400.145; registration No. 4001117).

### *Sample size calculation*

The sample size was determined using G\*Power 3.1 (Heinrich Heine University, Düsseldorf, Germany). Considering an effect size of 0.55 (8),  $\alpha = 0.05$ , and power of 80%, the sample size was calculated as  $n = 10$  per group.

### *Sample preparation*

Forty extracted bovine incisors free from cracks, caries, hypocalcification, or any structural defects were

selected for this study. Each tooth was sectioned into enamel blocks measuring approximately  $4 \times 6 \times 9$  mm, and embedded in methyl methacrylate resin. The enamel surfaces were then polished sequentially using silicon carbide papers under water irrigation to achieve a uniform baseline condition before the experiment.

Subsequently, the specimens were subjected to a pH-cycling protocol to induce subsurface enamel demineralization. The pH-cycling regimen was intended to simulate the natural fluctuations between demineralization and remineralization in the oral environment. During the demineralization phase, a buffered solution was used, consisting of 2.2 mM calcium chloride (Sigma-Aldrich, Germany), 2.2 mM sodium phosphate (Tappico, Iran), and 0.05 M acetic acid (Tappico). The pH of this solution was adjusted to 4.4 using 1 M potassium hydroxide (Sigma-Aldrich). The remineralizing solution consisted of 1.5 mM calcium chloride (Tappico), 0.9 mM sodium phosphate (Tappico), and 0.15 M potassium chloride (Shimi Caroon, Iran), with the pH adjusted to 7.0.

The specimens were immersed in 400 mL of the demineralizing solution for 12 hours. Subsequently, the teeth were transferred to the remineralizing solution for an additional 12 hours. This alternating demineralization–remineralization protocol was repeated daily for 14 consecutive days, with freshly prepared solutions used for each cycle. Upon completion of the cycling regimen, all specimens exhibited a characteristic frosty white appearance, confirming successful induction of subsurface enamel lesions.

### *Study groups*

The specimens were randomly assigned to four groups ( $n=10$ ), based on the type of resin infiltrant applied on demineralized enamel. The study groups were as follows:

Group 1 (G1; Commercial resin infiltrant): The specimens in this group were treated with a commercial resin infiltrant (ICON®; DMG, Hamburg, Germany).

Group 2 (G2; 5% BAG-modified infiltrant): Demineralized enamel samples were treated with an experimental resin infiltrant incorporating 5 wt% Bioglass® 45S5 (Sigma-Aldrich, MA, USA).

Group 3 (G3; 2% BAG-modified infiltrant): Demineralized enamel samples were treated with an experimental resin infiltrant incorporating 2 wt% Bioglass® 45S5.

Group 4 (G4: Filler-free infiltrant): Demineralized enamel samples were treated with the unfilled

experimental resin infiltrant. This resin was the same as that used in G2 and G3, but without Bioglass® 45S5. This group served as an additional control to evaluate the effect of filler incorporation.

#### Resin infiltrant formulation and application

The experimental resin infiltrant was formulated using bisphenol-A glycidyl methacrylate (Bis-GMA; Sigma-Aldrich, MA, USA), triethylene glycol dimethacrylate (Sigma-Aldrich), 2-hydroxyethyl methacrylate (Sigma-Aldrich), and ethanol (Sigma-Aldrich) at a weight ratio of 2:1:5:2, respectively. The monomers and solvent were accurately weighed using an analytical balance and transferred into glass vials to minimize light exposure during preparation.

For the BAG-containing formulations, 45S5 bioactive glass powder was incorporated into the resin matrix at concentrations of 2 wt% (G3) and 5 wt% (G2), calculated relative to the total resin weight. The predetermined amount of bioactive glass was gradually added to the pre-mixed monomer–ethanol system under continuous magnetic stirring to ensure uniform dispersion. The mixture was then homogenized by continuous magnetic stirring at room temperature for 48 hours to ensure complete dissolution and uniform dispersion of all components. After homogenization, the resin infiltrant was inspected to confirm the absence of phase separation and filler settling. The stability of the formulation was confirmed through light-protected storage at 4 °C until use, with no evidence of sedimentation or layer formation observed.

For all groups, demineralized enamel regions were etched with 37% phosphoric acid gel (Morvabon, Tehran, Iran) for 5 seconds, rinsed for 30 seconds and dried for 10 seconds. The ethanol 96% was then applied to the surface for two minutes to enhance resin infiltration. The surface was then air-dried for 10 seconds.

The resin infiltrant was applied and allowed to penetrate for 3 minutes while avoiding exposure to ambient light. The surface was polymerized for 40 seconds with an LED curing unit (Woodpecker, China) operating at an output intensity of 1200 mW/cm<sup>2</sup>.

#### Microhardness evaluation

After treatment, specimens were longitudinally sectioned and embedded with the cut surface exposed. The enamel surface was ground with 600–2000 grit silicon carbide papers (Matador, Tehran, Iran) to ensure uniform contact during microhardness testing. Vickers microhardness measurements were conducted using a Shimadzu HMV-2 microhardness tester (Shimadzu Corporation, Kyoto, Japan). A 10-N load was applied for 10 seconds at depths of 50, 100, and 150 µm from the enamel surface. Each depth was measured in triplicate, and the mean value was recorded.

#### Statistical analysis

The Shapiro–Wilk test confirmed normality of the data ( $P > 0.05$ ). A two-way ANOVA was performed to assess the effects of group, enamel depth, and their interaction on microhardness. When significant differences were detected, pairwise comparisons were performed using Tukey's honestly significant difference (HSD) post-hoc test. The significance level was set at  $P < 0.05$ .

### Results

Table 1 presents the mean and standard deviation (SD) of microhardness at different depths in the study groups. G1 (ICON®) exhibited the highest microhardness, while G4 (the filler-free infiltrant) showed the lowest value at all depths. A two-way ANOVA revealed a significant interaction between the variables ( $P = 0.041$ ); therefore, comparisons were conducted using one-way ANOVA and repeated measures analysis. (Figure 1)

ANOVA revealed a significant difference in microhardness among the study groups at all depths ( $P < 0.001$ ; Table 1). Tukey's HSD test showed that G1 had significantly greater microhardness than the other groups at all depths ( $P < 0.05$ ; Table 1).

At a depth of 50 µm, microhardness was significantly greater in G2 (5% BAG-modified infiltrant) than G3 (2%

**Table 1.** Mean and standard deviation (SD) of microhardness (µm) at different depths in the study groups

Group	50 microns	100 microns	150 microns	P-value
	Mean ± SD	Mean ± SD	Mean ± SD	
G1	242.0 ± 31.5 <sup>aA</sup>	304.8 ± 39.0 <sup>aB</sup>	335.0 ± 26.5 <sup>aC</sup>	<0.001
G2	172.0 ± 35.0 <sup>bA</sup>	245.0 ± 51.1 <sup>bB</sup>	308.1 ± 28.4 <sup>bC</sup>	<0.001
G3	95.4 ± 23.2 <sup>cA</sup>	225.5 ± 48.0 <sup>bcB</sup>	310.2 ± 52.3 <sup>bcC</sup>	<0.001
G4	90.6 ± 25.5 <sup>cA</sup>	202.2 ± 47.5 <sup>cB</sup>	255.2 ± 39.6 <sup>cC</sup>	<0.001
P-value	<0.001	<0.001	<0.001	

Different capital letters indicate statistically significant differences between depths at  $P < 0.05$ .

Different lowercase letters indicate statistically significant differences between groups at  $P < 0.05$ .

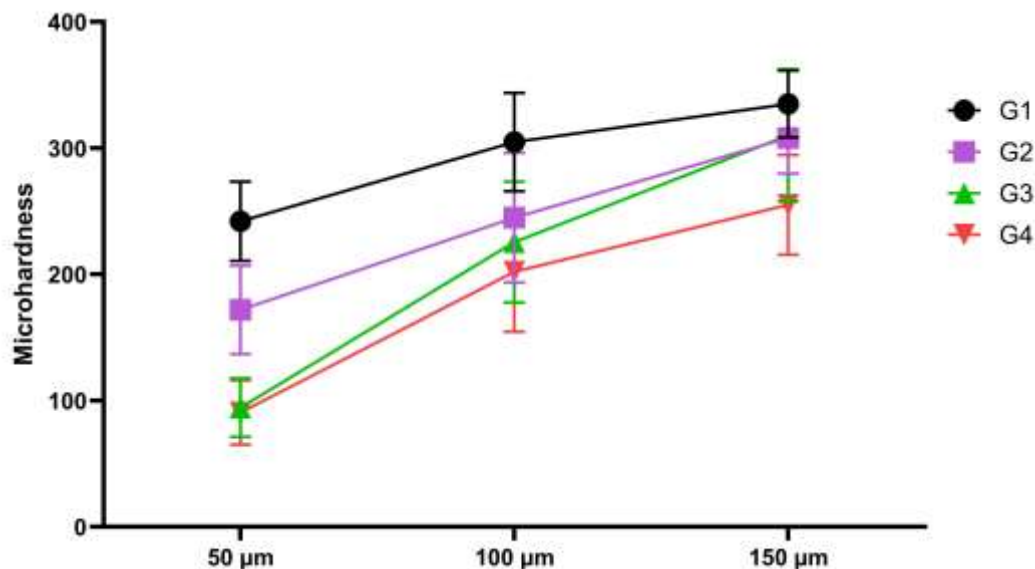


**Figure 1.** The average microhardness values observed in the study groups at different depths.

BAG-modified infiltrant) and G4 ( $P < 0.05$ ; Table 1), which were statistically comparable ( $P > 0.05$ ).

At 100  $\mu\text{m}$ , G2 exhibited significantly greater microhardness than G4 ( $P < 0.05$ ; Table 1), while G3 showed no significant difference compared to either G2 or G4 ( $P > 0.05$ ).

At 150  $\mu\text{m}$ , microhardness in G2 and G3 was comparable ( $P > 0.05$ ), and both were significantly higher than in G4 ( $P < 0.05$ ).

The repeated measures analysis showed a significant increase in microhardness with increasing depth in all groups ( $P < 0.001$ ; Table 1), with significant differences observed between all depths ( $P < 0.05$ ).

## Discussion

This study evaluated the effect of incorporating 45S5 bioactive glass into resin infiltrants on the microhardness recovery of artificially demineralized enamel at various subsurface depths.

In the present study, ICON® (G1) demonstrated the highest microhardness values at all evaluated depths, significantly outperforming both the BAG-modified (G2 and G3) and filler-free (G4) experimental formulations. ICON® is a commercial resin infiltrant widely used for treatment of WSLs. It is a low-viscosity, TEGDMA-based (triethylene glycol dimethacrylate) resin matrix without inorganic fillers, thus demonstrating suitable penetration depth.

The results of this study are in line with previous laboratory and clinical studies, which have shown that ICON® is highly effective in enhancing mechanical properties and improving esthetic outcomes in early

enamel lesions by deeply infiltrating and sealing the lesion body (8, 9, 12, 13, 23-25). The superior performance of ICON® compared to experimental resin infiltrants used in this study can be attributed to its low-viscosity, TEGDMA-based formulation, which allows for more thorough saturation of the lesion body compared to the more viscous experimental systems (26, 27).

At 50  $\mu\text{m}$  depth, the experimental resin formulation containing 5 wt% Bioglass® 45S5 (G2) showed significantly greater microhardness than both G3 (experimental resin containing 2 wt% Bioglass® 45S5) and G4 (filler-free infiltrant). At the depth of 100  $\mu\text{m}$ , G2 had significantly greater microhardness than G4, whereas at 150  $\mu\text{m}$ , microhardness of G2 and G3 were comparable to each other and significantly greater than G4. These findings showed that incorporation of Bioglass® 45S5 into the resin infiltrant was effective in enhancing the mineral content of demineralized enamel. Increasing the concentration of Bioglass® 45S5 also caused a significant increase in microhardness, which was significant at the most superficial depth (50  $\mu\text{m}$ ).

The experimental infiltrants in this study incorporated Bis-GMA (a more viscous, hydrophobic monomer) and bioactive glass filler. The incorporation of Bis-GMA increased viscosity, restricting resin flow into deep intercrystalline spaces and resulting in incomplete pore occlusion, particularly in the deeper lesion body regions (100–150  $\mu\text{m}$ ). Consequently, even though bioactive glass releases calcium and phosphate ions, these ions can only enhance hardness recovery in regions successfully infiltrated by resin. The incomplete infiltration in experimental groups, combined with

limited ion diffusion pathways, resulted in reduced microhardness recovery compared to the ICON® group (9, 28). The present findings imply that while BAG provides benefits over unfilled controls, viscosity-related limitations prevent BAG-containing formulations from matching ICON®'s performance across the entire lesion depth range.

In the present study, all infiltrants, including ICON® and the BAG-modified formulations, were applied using a standard single-application protocol. In contrast, Paris et al. (12) demonstrated that repeated infiltrant application significantly increased microhardness. It is possible that multiple infiltration applications could potentially enhance BAG-related remineralization by increasing both the penetration depth and the amount of bioactive filler delivered within the lesion body.

Microhardness demonstrated a statistically significant increase with measurement depth across all groups. The subsurface lesion body (50-100 µm) tends to be more heavily demineralized and porous, whereas the deeper enamel (100-150 µm) retains higher mineral density, making it less susceptible to acid dissolution (10). This accounts for the observed higher microhardness at 150 µm compared to 100 and 50 µm depths across all groups. Similar depth-dependent patterns have been documented in previous studies examining lesion progression and remineralization effects of various agents (29, 30).

The higher microhardness observed in groups containing Bioglass® 45S5 compared to filler-free infiltrant is consistent with findings of Park et al. (23) and de Cerqueira et al. (31), who demonstrated that incorporating Bioglass 45S5 into resin matrices enhances mechanical recovery through sustained  $\text{Ca}^{2+}/\text{PO}_4^{3-}$  ion release and subsequent hydroxyapatite precipitation. These studies also reported greater hardness improvements at deeper lesion depths, consistent with the depth-dependent trends observed in the present study.

Bioglass® 45S5 releases  $\text{Ca}^{2+}$ ,  $\text{PO}_4^{3-}$ , and  $\text{Si}(\text{OH})_4$  ions upon contact with aqueous media, which raises the local pH and promotes the formation of an apatite-like phase. Such apatite-like structure can occlude enamel porosities and reinforce demineralized tissue (32). Recent studies have focused on developing bioactive resin infiltrants that combine effective lesion penetration with sustained ion release to enhance both mechanical strength and biological remineralization (22, 29, 32-35).

When comparing G2 and G3 to each other, a significant difference in microhardness was observed

only at a depth of 50 µm. With increasing depths to 100 µm and 150 µm, these two groups did not show a significant difference from each other. This likely reflects that a higher filler loading increases resin viscosity, impairing capillary penetration (16), and potentially causes uneven particle dispersion or agglomeration, which limits ion release in the deeper lesion areas (37, 38).

This study has some limitations. The in vitro pH-cycling model cannot fully replicate the biological complexity of the oral environment, which influences the behavior and progression of natural enamel lesions (40, 41). Additionally, bovine enamel was used as the substrate in this study. Although bovine enamel closely resembles human enamel in composition, microhardness, and permeability, it is not entirely identical to human enamel (42, 43). These structural differences may influence lesion progression and resin infiltration behavior, and should be considered when extrapolating the results to clinical conditions. Future studies should explore resin penetration depth, degree of conversion, ion-release profile, and evidence of apatite formation after applying different formulations of resin infiltrants on demineralized enamel. Further research is also warranted to investigate alternative formulations or filler concentrations to enhance remineralization effectiveness.

## Conclusions

Under the conditions used in this study:

- 1- Resin infiltrant formulation and lesion depth significantly influenced enamel microhardness recovery.
- 2- ICON® achieved the highest microhardness values at all evaluated depths, significantly outperforming all experimental formulations.
- 3- Microhardness increased with depth in all groups.
- 4- Incorporation of Bioglass® 45S5 into the resin infiltrant was effective in enhancing mineral content of demineralized enamel, as compared to unfilled resin. Increasing the concentration of Bioglass® 45S5 also caused a significant rise in microhardness at 50 µm depth, but comparable results at 100 and 150 µm depths.

## Acknowledgements

The authors sincerely thank the staff of the Restorative and Cosmetic Dentistry Department for their valuable cooperation.

## Conflicts of interest

The authors declare no conflict of interest.

## Ethical considerations

This study was approved by the ethics committee of Mashhad University of Medical Sciences, Mashhad, Iran (IR.MUMS.DENTISTRY.REC.1400.145; registration No. 4001117).

## Author contributions

H.H. and H.B. contributed to the study design and data interpretation; H.B., K.J. and M.V. contributed to the conceptualization of the study, data analysis, and manuscript editing; A.A., K.J., and M.V. contributed to data collection and manuscript preparation. All authors approved the final manuscript.

## Funding

This study was conducted with the financial support of the Vice Chancellor for Research of Mashhad University of Medical Sciences with Grant Number 4001117.

## References

1. Anil A, Ibraheem WI, Meshni AA, Preethanath R, Anil S. Demineralization and remineralization dynamics and dental caries. *Dental Caries-The Selection of Restoration Methods and Restorative Materials: IntechOpen*; 2022.
2. Enax J, Fandrich P, Schulze zur Wiesche E, Epple M. The remineralization of enamel from saliva: A chemical perspective. *Dent J (Basel)* 2024;12(11):339.
3. Abou Neel EA, Aljabo A, Strange A, Ibrahim S, Coathup M, Young AM, et al. Demineralization–remineralization dynamics in teeth and bone. *Int J Nanomedicine* 2016;4743–4763.
4. Roberts WE, Mangum JE, Schneider PM. Pathophysiology of demineralization, part II: Enamel white spots, cavitated caries, and bone infection. *Curr Osteoporos Rep* 2022;20(1):106–119.
5. Lopes PC, Carvalho T, Gomes AT, Veiga N, Blanco L, Correia MJ, et al. White spot lesions: diagnosis and treatment—a systematic review. *BMC Oral Health* 2024;24(1):58.
6. Manoharan V, Arun Kumar S, Arumugam SB, Anand V, Krishnamoorthy S, Methippara JJ. Is Resin Infiltration a Microinvasive Approach to White Lesions of Calcified Tooth Structures?: A Systemic Review. *Int J Clin Pediatr Dent* 2019;12(1):53–58.
7. Knösel M, Eckstein A, Helms HJ. Durability of esthetic improvement following Icon resin infiltration of multibracket-induced white spot lesions compared with no therapy over 6 months: a single-center, split-mouth, randomized clinical trial. *Am J Orthod Dentofacial Orthop* 2013;144(1):86–96.
8. Paris S, Schwendicke F, Seddig S, Müller WD, Dörfer C, Meyer-Lueckel H. Micro-hardness and mineral loss of enamel lesions after infiltration with various resins: influence of infiltrant composition and application frequency in vitro. *J Dent* 2013;41(6):543–548.
9. Meyer-Lueckel H, Paris S. Improved resin infiltration of natural caries lesions. *J Dent Res* 2008;87(12):1112–1116.
10. ten Cate JM. Remineralization of deep enamel dentine caries lesions. *Aust Dent J* 2008;53(3):281–285.
11. Fang P, Ye X, Tian L, Chen Y, Li X, Hu H. Modified casein-stabilized amorphous calcium phosphate nanoparticles prevent dental caries by inhibiting the growth of *Streptococcus mutans* and promoting the remineralization of tooth enamel. *Colloids Surf B Biointerfaces* 2025;114815.
12. Paris S, Schwendicke F, Keltsch J, Dörfer C, Meyer-Lueckel H. Masking of white spot lesions by resin infiltration in vitro. *J Dent* 2013;41(5):28–34.
13. Soveral M, Machado V, Botelho J, Mendes JJ, Manso C. Effect of Resin Infiltration on Enamel: A Systematic Review and Meta-Analysis. *J Funct Biomater* 2021;12(3).
14. Li M, Yang Z, Huang Y, Li Y, Zhou Z. In vitro effect of resin infiltrant on resistance of sound enamel surfaces in permanent teeth to demineralization. *PeerJ* 2021;9:e12008.
15. Yazkan B, Ermis RB. Effect of resin infiltration and microabrasion on the microhardness, surface roughness and morphology of incipient carious lesions. *Acta Odontol Scand* 2018;76(7):473–481.
16. Ahmed SZ, Khan AS, Nasser WW, Alrushaid MA, Alfaraj ZM, Aljeshi MM, et al. Physio-Mechanic and Microscopic Analyses of Bioactive Glass-Based Resin Infiltrants. *Microsc Res Tech* 2025;88(2):595–610.
17. Borges R, Santos KF, Pelosini AM, Ferraz EP, Cesar PF, Marchi J. Bioceramics and Bioactive Glasses for Tooth Repair and Regeneration. *Bioceramics: Status in Tissue Engineering and Regenerative Medicine (Part 2): Bentham Science Publishers*; 2024. p. 221–260.
18. Hench LL. The story of Bioglass. *J Mater Sci Mater Med* 2006;17(11):967–978.
19. Khan AS, AlDahlan BG, Maghrabi NH, Albilali HW, Ahmed SZ, Shah AT, et al. Application of laser on enamel surface with three types of bioactive glasses-based resin infiltrants: an in vitro study. *J Mech Behav Biomed Mater* 2023;141:105792.
20. Shen H, Wang B, Shen Z, Xie Z, Zhang J, Wang C, et al. Cerium-Containing Mesoporous Bioactive Glass Nanoparticles Doped Resin Infiltrants: Synergistic Mechanical Reinforcement and Bioactive Therapy for Early Caries Management. *Ceramics International* 2025;51(27): 53782–53795.
21. Diniz AC, Bauer J, Veloso SdAR, Abreu-Pereira CA, Carvalho CN, Leitão TJ, et al. Effect of bioactive filler addition on the mechanical and biological properties of resin-modified glass ionomer. *Materials* 2023;16(5):1765.

22. Wang H, Wu J, Zhang H, Li A, Qiu D, Dong Y. Fabricating a novel bioactive resin Infiltrant to treat white spot lesions of enamel. *J Dent* 2025;158:105815.
23. Park IS, Kim HJ, Kwon J, Kim DS. Comparative In Vitro Study of Sol-Gel-Derived Bioactive Glasses Incorporated into Dentin Adhesives: Effects on Remineralization and Mechanical Properties of Dentin. *J Funct Biomater* 2025;16(1):29.
24. Mazzitelli C, Josic U, Maravic T, Mancuso E, Goracci C, Cadenaro M, et al. An Insight into Enamel Resin Infiltrants with Experimental Compositions. *Polymers (Basel)* 2022;14(24).
25. Boruziniat A, Ahrari F, Shafaei H, Faravani F, Rangrazi A, Akbari Kamrani F, et al. The Efficacy of Various Conditioning Methods in Restoring the Color of White Spot Lesions Through Resin Infiltration: Er,Cr:YSGG laser for resin infiltration. *J Lasers Med Sci* 2025;16:e60.
26. Kielbassa AM, Summer S, Frank W, Lynch E, Batzer J-S. Equivalence study of the resin-dentine interface of internal tunnel restorations when using an enamel infiltrant resin with ethanol-wet dentine bonding. *Sci Rep* 2024;14(1):12444.
27. Srikumar GPV, Ghosh M, Kumar AA, Bardia S, Wasule A, Beutlin JS. An in vitro evaluation of Icon resin infiltrant penetration into demineralized enamel lesions using an indirect staining technique with confocal laser scanning microscope analysis in dual fluorescence mode. *J Conserv Dent Endod* 2024;27(4):366–372.
28. El Meligy O, Alamoudi NM, Eldin Ibrahim ST, Felemban OM, Al-Tuwirqi AA. Effect of resin infiltration application on early proximal caries lesions in vitro. *J Dent Sci* 2021;16(1):296–303.
29. Prada AM, Potra Cicalău GI, Ciavoi G. A Review of White Spot Lesions: Development and Treatment with Resin Infiltration. *Dent J (Basel)* 2024;12(12).
30. Ooi HL, Bartlett D, Almansour A, LeBlanc A, White D, Morrell A, et al. Beyond the Surface: Mechanical and Porosity Gradients in Eroded Enamel. *J Dent Res* 2025;220345251385464.
31. de Cerqueira GA, Damasceno JE, Pedreira PR, Souza AF, Aguiar FHB, Marchi GM. Roughness and microhardness of demineralized enamel treated with resinous infiltrants and subjected to an acid challenge: an in vitro study. *The Open Dentistry Journal* 2023;17(1).
32. Choi J-W, Han AR, Yang S-Y. Ion release and apatite formation of resin based pit and fissure sealants containing 45S5 bioactive glass. *Polymers* 2024;16(13):1855.
33. Yun J, Burrow MF, Matinlinna JP, Wang Y, Tsoi JKH. A Narrative Review of Bioactive Glass-Loaded Dental Resin Composites. *J Funct Biomater* 2022;13(4).
34. Han X, Chen Y, Jiang Q, Liu X, Chen Y. Novel Bioactive Glass-Modified Hybrid Composite Resin: Mechanical Properties, Biocompatibility, and Antibacterial and Remineralizing Activity. *Front Bioeng Biotechnol* 2021;9:661734.
35. Seifi M, Eskandarloo F, Amdjadi P, Farmany A. Investigation of mechanical properties, remineralization, antibacterial effect, and cellular toxicity of composite orthodontic adhesive combined with silver-containing nanostructured bioactive glass. *BMC Oral Health* 2024;24(1):650.
36. Ahmed SZ, Khan AS, Alshehri M, Alsebaa F, Almutawah F, Mohammed Aljeshi M, et al. In-vitro comparative thermo-chemical aging and penetration analyses of bioactive glass-based dental resin infiltrates. *PeerJ* 2025;13:e18831.
37. Ahmed SZ, Khan AS, Aljeshi NM, Md Sabri BA, Akhtar S, Abu Hassan MI. A Comparative In Vitro Physicochemical Analysis of Resin Infiltrants Doped With Bioactive Glasses. *Cureus* 2024;16(7):e64500.
38. Chabuk MM, Al-Shamma AM. Surface roughness and microhardness of enamel white spot lesions treated with different treatment methods. *Heliyon* 2023;9(7):e18283.
39. Meng Q, Wang Y, He J, Chen L, Meng J, Lyons K, et al. The effect of combined use of resin infiltration with different bioactive calcium phosphate-based approaches on enamel white spot lesions: An in vitro study. *J Dent* 2024;143:104909.
40. Buzalaf MA, Hannas AR, Magalhães AC, Rios D, Honório HM, Delbem AC. pH-cycling models for in vitro evaluation of the efficacy of fluoridated dentifrices for caries control: strengths and limitations. *J Appl Oral Sci* 2010;18(4):316–334.
41. Fu Y, Ekambaram M, Li KC, Zhang Y, Cooper PR, Mei ML. In Vitro Models Used in Cariology Mineralisation Research-A Review of the Literature. *Dent J (Basel)* 2024;12(10).
42. Arango-Santander S, Montoya C, Pelaez-Vargas A, Ossa EA. Chemical, structural and mechanical characterization of bovine enamel. *Arch Oral Biol* 2020;109:104573.
43. Yassen GH, Platt JA, Hara AT. Bovine teeth as substitute for human teeth in dental research: a review of literature. *J Oral Sci* 2011;53(3):273–282.